

Electronic Supplementary Information (ESI) for

**Unveiling the impurity-modulated photoluminescence from Mn²⁺-
containing metal chalcogenide semiconductor via Fe²⁺ doping**

Zhiqiang Wang,^a Yong Liu,^a Jiaxu Zhang,^a Xiang Wang,^a Zhou Wu,^a Jin Wu,^a Ning Chen,^a Dong-sheng Li,^c
and Tao Wu*^b

^a College of Chemistry, Chemical Engineering and Materials Science, Soochow University, Jiangsu 215123, China.

^b College of Chemistry and Materials Science, Guangdong Provincial Key Laboratory of Functional Supramolecular Coordination Materials and Applications, Jinan University, Guangzhou 510632, China.

^c College of Materials and Chemical Engineering, Hubei Provincial Collaborative Innovation Centre for New Energy Microgrid, Key Laboratory of Inorganic Nonmetallic Crystalline and Energy Conversion Materials, China Three Gorges University, Yichang 443002, China.

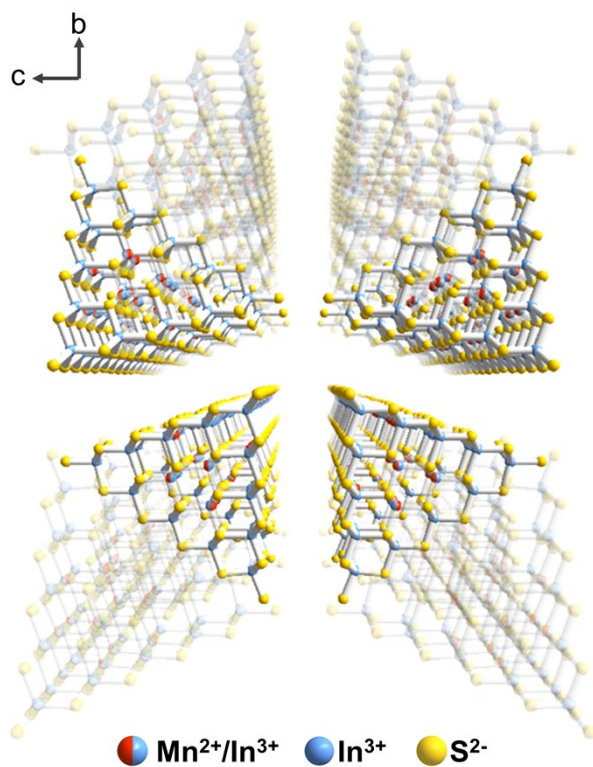


Figure S1. Assembly of T5-MnInS cluster-based one-dimensional metal chalcogenides. Note: Positively-charged protonated organic amines around each cluster are omitted for clarity.

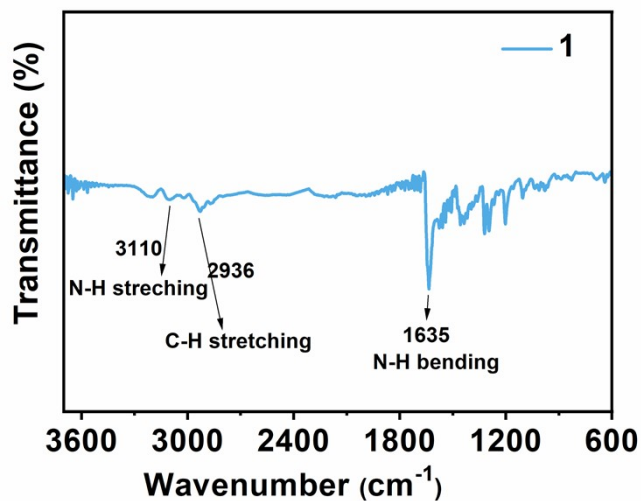


Figure S2. FTIR spectrum of **1**. Stretching and bending modes of N-H as well as stretching mode of C-H are displayed, indicating the existence of organic amines in **1**.

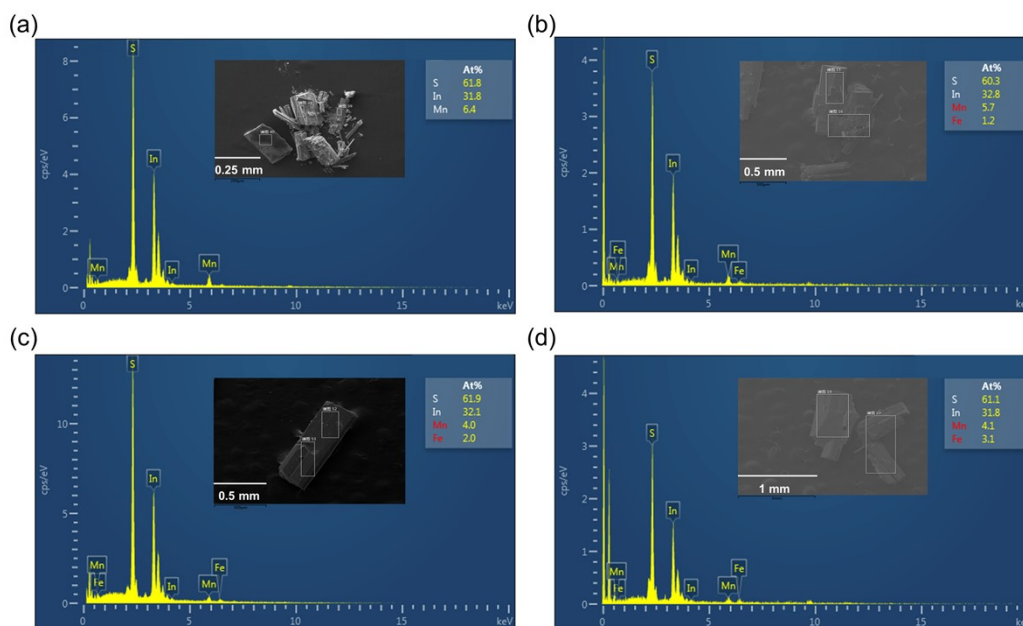


Figure S3. Energy dispersive spectroscopy (EDS) of (a) **1**, (b) **1-A**, (c) **1-B**, and (d) **1-C**. The inserts are SEM images of corresponding as-synthesized microcrystal samples. For **1**, the atom ratio of In : Mn is near 5 : 1, being in accordance with the SCXRD results. The actual corresponding ratios of Fe : Mn atom number are 1.2 : 5.7, 2.0 : 4.0 and 3.1 : 4.1 for **1-A**, **1-B**, and **1-C**, respectively, which suggest the doping level of averagely 1, 2 and 3 Fe²⁺ ions per T5 cluster, respectively. Thus, the chemical formulas of Fe²⁺-doped samples mentioned above can be estimated to be [Fe_{1.04}Mn_{4.96}In₂₈S₅₅]-6.6(H⁺-DBU)-3.7(2H⁺-TMEDA), [Fe₂Mn₄In₂₈S₅₅]-6.6(H⁺-DBU)-3.7(2H⁺-TMEDA) and [Fe_{2.6}Mn_{3.4}In₂₈S₅₅]-6.6(H⁺-DBU)-3.7(2H⁺-TMEDA), respectively.

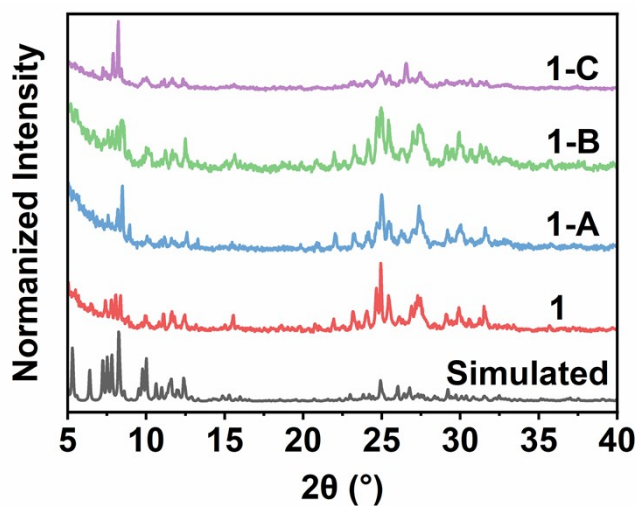


Figure S4. Powder XRD patterns of **1** and Fe²⁺-doped samples (**1-A**, **1-B**, and **1-C**) as well as the simulated PXRD patterns.

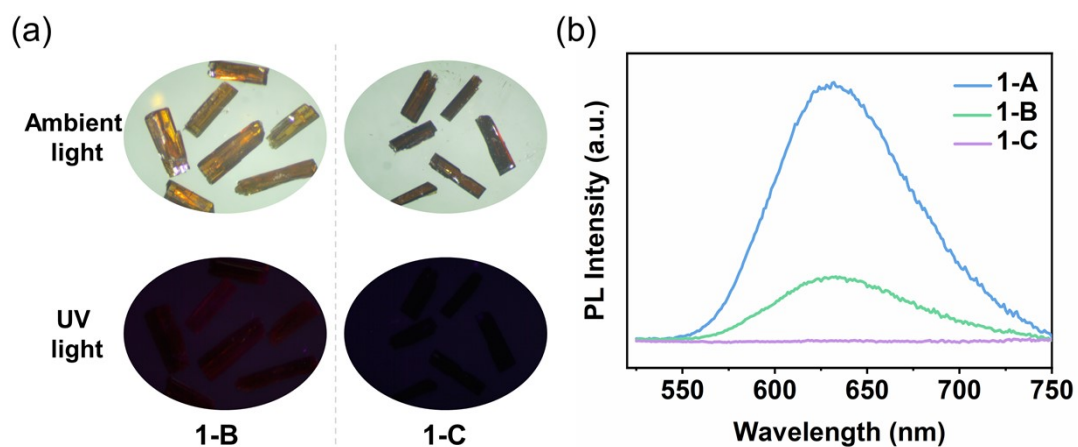


Figure S5. (a) Optical photographs of **1-B** and **1-C** under either ambient light or 365 nm excitation. As is from our naked eyes, single crystals of **1-B** show very weak red PL emission, while **1-C** shows no emission. (b) The steady-state PL spectra of **1-A**, **1-B**, and **1-C**.

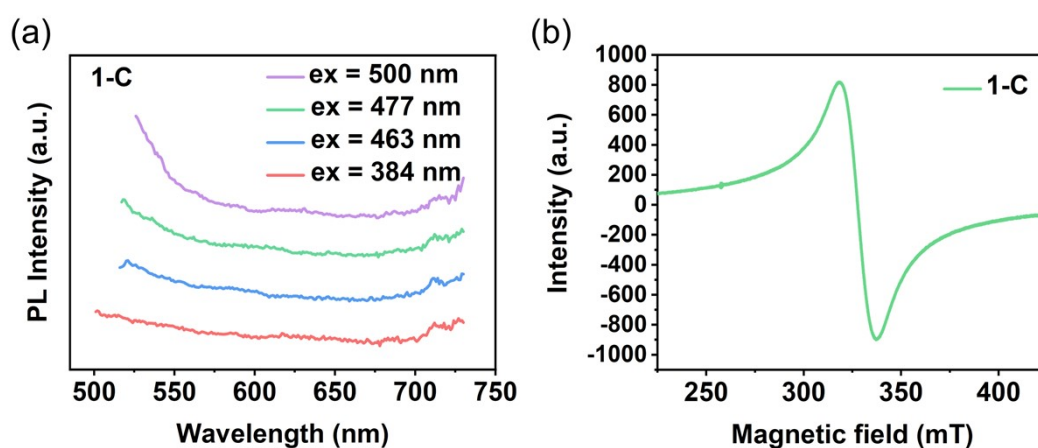


Figure S6. (a) Room-temperature steady-state PL spectra of **1-C** under varied excitation wavelength. (b) Electron paramagnetic resonance spectrum (EPR) of **1-C**. The broad signal is an indication of Mn···Mn coupling interaction.

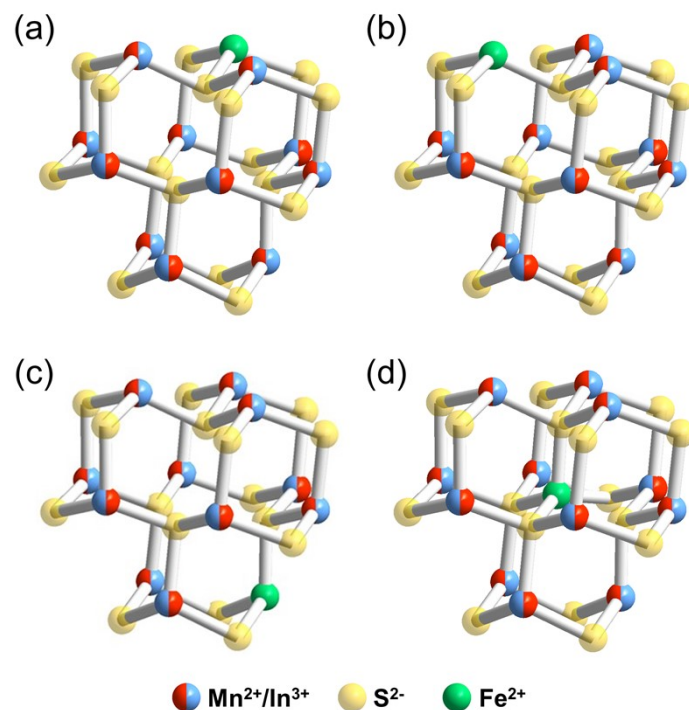


Figure S7. Schematic illustration of the core region in Fe^{2+} -doped T5-MnInS cluster with one Mn^{2+} ion substituted by one Fe^{2+} ion. 12 $\text{Mn}^{2+}/\text{In}^{3+}$ mixed sites are homogeneously distributed at four faces of T5 cluster. Hence, Figure (a-c) represent the doping of 1 Fe^{2+} impurity at one face of T5 cluster, respectively. Figure (d) displays the possible Fe^{2+} impurity doping into the void center site due to the slightly smaller radius of Fe^{2+} (74 pm) than that of Mn^{2+} (80 pm). In a word, **1-A** with averagely one Fe^{2+} ion in each T5 cluster ensures the strong $\text{Mn}\cdots\text{Mn}$ and $\text{Mn}\cdots\text{Fe}$ coupling interactions.

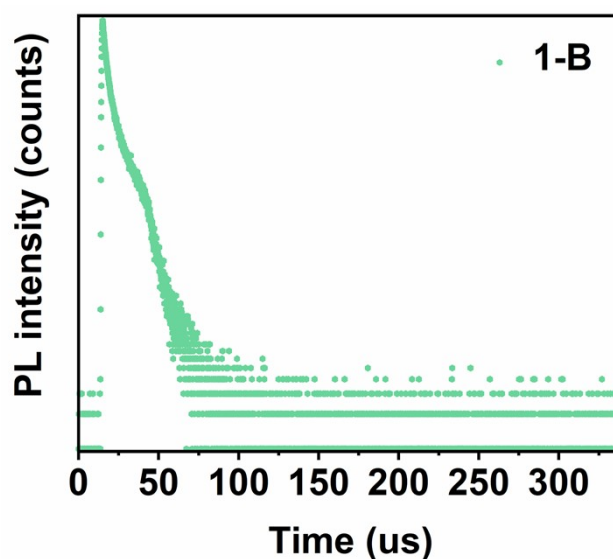


Figure S8. PL decay curve of **1-B** (excited at 384 nm and measured at 634 nm).

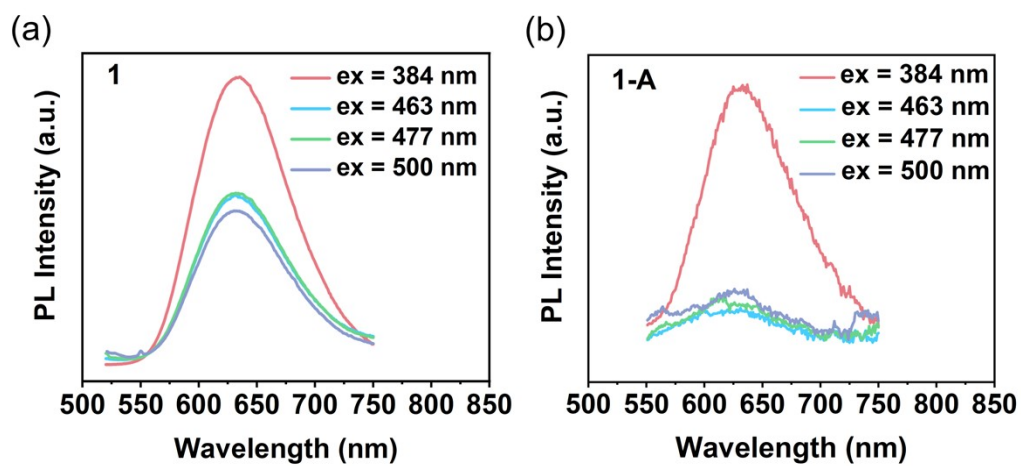


Figure S9. PL spectra of **1** and **1-A** at different excitation wavelength.

Table S1. Structure refinement parameters on **1**.

Compound	1
Empirical formula of framework	In ₂₈ Mn ₆ S ₅₅ C _{81.6} H _{178.8} N _{20.6}
Formula weight	5307.90
CCDC number	2012861
Crystal system	orthorhombic
Space group	<i>Cmcm</i>
Z	8
<i>a</i> (Å)	19.508(10)
<i>b</i> (Å)	46.77(2)
<i>c</i> (Å)	42.60(3)
α (deg.)	90
β (deg.)	90
γ (deg.)	90
<i>V</i> (Å ³)	38870(40)
GOF on <i>F</i> ²	1.067
<i>R</i> ₁ , <i>wR</i> ₂ (<i>I</i> > 2 σ (<i>I</i>))	0.0632, 0.1897
<i>R</i> ₁ , <i>wR</i> ₂ (all data)	0.0794, 0.2153

Table S2. Fitting details of PL decays of **1**, **1-A**, and **1-B** (excited at 384 nm and measured at 634 nm).

	1	1-A	1-B
τ_1	29.35 us / 76.8%	14.41 us / 82.30%	10 us / 71.24%
τ_2	90.35 us / 23.2%	3.24 us / 17.7%	1.8 us / 28.76%
τ_{ave}	43.5 us	12.4 us	7.65 us

Table S3. The fitting details of Mn²⁺-related PL decay curves of **1** detected at 634 nm under varied excitation wavelength.

	Ex = 384 nm	Ex = 463 nm	Ex = 477 nm	Ex = 500 nm
τ_1	29.35 us / 76.8%	26.7 us / 78.92%	26.4 us / 77.09%	28.27 us / 81.22%
τ_2	90.35 us / 23.2%	74.86 us / 21.08%	69.68 us / 22.91%	75.63 us / 18.78%
τ_{av}	43.5 us	36.85 us	36.32 us	37.16 us
e				

Table S4. The fitting details of Mn²⁺-related PL decay curves of **1-A** detected at 634 nm under varied excitation wavelength.

	Ex = 384 nm	Ex = 463 nm	Ex = 477 nm	Ex = 500 nm
τ_1	14.41 us / 82.30%	12.82 us / 79.13%	12.83 us / 79.26%	12.68 us / 82.93%
τ_2	3.24 us / 17.70%	1.77 us / 20.87%	1.88 us / 20.74%	1.84 us / 17.07%
τ_{av}	12.4 us	10.5 us	10.56 us	10.8 us

e
